

28p

CONFIDENTIAL

5574148 P30
Copy 586

NASA TM X-441

NASA TM X-441



~~N 63 16140~~

N 63 16140

Classification Changed to
Declassified Effective 18 April 1963
Authority NASA CON-3 By J.J. Carroll

code-1

TECHNICAL MEMORANDUM

X-441

STABILITY AND CONTROL CHARACTERISTICS AT A MACH NUMBER
OF 2.01 OF A SUPERSONIC VTOL AIRPLANE MODEL HAVING
A BROAD FUSELAGE AND SMALL DELTA WINGS

By Cornelius Driver and M. Leroy Spearman

Langley Research Center
Langley Field, Va.

OTS PRICE	
XEROX	\$
MICROFILM	\$

CLASSIFIED DOCUMENT - TITLE UNCLASSIFIED

This material contains information affecting the national defense of the United States within the meaning of the espionage laws, Title 18, U.S.C., Secs. 793 and 794, the transmission or revelation of which in any manner to an unauthorized person is prohibited by law.

NATIONAL AERONAUTICS AND SPACE ADMINISTRATION
WASHINGTON
February 1961

CONFIDENTIAL

CONFIDENTIAL

NATIONAL AERONAUTICS AND SPACE ADMINISTRATION

TECHNICAL MEMORANDUM X-441

STABILITY AND CONTROL CHARACTERISTICS AT A MACH NUMBER

OF 2.01 OF A SUPERSONIC VTOL AIRPLANE MODEL HAVING

A BROAD FUSELAGE AND SMALL DELTA WINGS*

By Cornelius Driver and M. Leroy Spearman

SUMMARY

An investigation has been conducted in the Langley 4- by 4-foot supersonic pressure tunnel at a Mach number of 2.01 to determine the stability and control characteristics of a model representative of a supersonic vertical-take-off-and-landing airplane. The model had a broad fuselage, small delta wings, and twin vertical tails.

The results indicated that the body alone provides a reasonably high lift-curve slope and a maximum value of lift-drag ratio of about 4. This value was increased to about 5.2 by the addition of the wings. The complete configuration indicated a positive value of pitching moment at zero lift such that positive deflections of the elevator would be required for trimming in the lower lift range. However, because of a reduction in stability at higher lifts, a slight forward movement of the center of gravity may be necessary.

The configuration displayed an initially low value of directional stability that decreased rapidly with increasing angle of attack until directional instability occurred above an angle of 6° . In addition, the configuration had a positive dihedral effect that increased with increasing angle of attack.

INTRODUCTION

Among the manned aircraft currently being proposed are those that combine the features of supersonic operation with the ability to take off and land vertically (VTOL). Some of the configurations being considered make use of lifting fans in order to achieve the VTOL capability. If these fans are installed in the body, the result may be a rather broad

*Title, Unclassified.

CONFIDENTIAL

flat-type fuselage that might be expected to have a pronounced effect on the aerodynamic characteristics of the vehicle. Accordingly, an investigation has been undertaken in the Langley 4- by 4-foot supersonic pressure tunnel to determine the aerodynamic characteristics at a Mach number of 2.01 of a model representative of a supersonic VTOL airplane having a broad fuselage, small delta wings, and twin vertical tails. The results of the investigation, together with a limited analysis, are presented herein.

SYMBOLS

All data presented herein are referred to the body system of axes except the lift and drag data which are referred to the stability system of axes. The moment reference point is at a longitudinal station corresponding to 65.35 percent of the body length (40 percent wing mean aerodynamic chord).

b	wing span, 1.77 ft
C_D	drag coefficient, $\frac{\text{Drag}}{qS}$
C_L	lift coefficient, $\frac{\text{Lift}}{qS}$
C_Y	side-force coefficient, $\frac{\text{Side force}}{qS}$
$C_{Y\beta}$	side-force parameter
C_l	rolling-moment coefficient, $\frac{\text{Rolling moment}}{qSb}$
$C_{l\beta}$	effective-dihedral parameter
C_m	pitching-moment coefficient, $\frac{\text{Pitching moment}}{qS\bar{c}}$
C_n	yawing-moment coefficient, $\frac{\text{Yawing moment}}{qSb}$

$C_{n\beta}$	directional-stability parameter
c	local chord, ft
\bar{c}	wing mean aerodynamic chord, 1.08 ft
q	free-stream dynamic pressure, lb/sq ft
S	wing area, 1.488 sq ft
α	angle of attack, deg
β	angle of sideslip, deg
δ_e	elevator deflection, deg
δ_r	rudder deflection, deg

Subscripts:

L	left
R	right

Model components:

B	body
V	vertical tail
W	wing

MODEL AND APPARATUS

Details of the model are shown in figure 1 and the geometric characteristics are given in table I. The model was constructed in such a way that the wing and tail panels could be removed and the deflection angles of the elevator and rudder could be changed. Both a plane and a cambered wing were investigated. The body was designed to provide for an internal flow system composed of twin horizontal-ramp inlets on the sides of the body that were ducted to six simulated jet exits side by side at the base of the body. No attempt was made to simulate jet exits that might be required for VTOL, however. With but one exception, all tests were made with 0.10-inch-wide transition strips of No. 80 carborundum grains affixed 2 inches behind the fuselage nose and at the 10-percent-chord stations of the wing and tail surfaces.

The model was mounted in the tunnel on a remote-controlled rotary sting. Six-component force and moment measurements were made through the use of an internal strain-gage balance.

TESTS, CORRECTIONS, AND ACCURACY

The tests were made in the Langley 4- by 4-foot supersonic pressure tunnel with the following test conditions:

Mach number	2.01
Stagnation temperature, °F	110
Stagnation pressure, lb/sq in.	10
Reynolds number, based on \bar{c}	2.6×10^6

The stagnation dewpoint was maintained sufficiently low (-25° F or less) so that no condensation effects were encountered in the test section.

Tests were made for an angle-of-attack range of about -7° to 16° at $\beta \approx 0^\circ$ and for an angle-of-sideslip range of about -8° to 12° at $\alpha = -0.5^\circ$ and about -8° to 1° at $\alpha = 4.8^\circ, 9.3^\circ, \text{ and } 13.8^\circ$.

The angles of attack and sideslip were corrected for deflection of the balance and sting under load. The drag data have been corrected for the effects of internal flow, base pressure, and balance chamber pressure.

The estimated accuracy of the individual measured quantities is as follows:

C_L	± 0.0004
C_D	± 0.0007
C_m	± 0.0004
C_n	± 0.0001
C_l	± 0.0003
C_y	± 0.0007
α , deg	± 0.2
β , deg	± 0.2

The control deflections were accurate to within $\pm 0.1^\circ$.

DISCUSSION

The addition of transition strips to the complete configuration with the cambered wing (fig. 2) had little effect on the aerodynamic characteristics in pitch other than to cause a slight increase in drag with an attendant decrease in lift-drag ratio. All the other results presented herein were obtained with transition fixed.

The primary effects of cambering the wing (fig. 3) were to cause a positive increment in C_m , to increase the minimum value of C_D , and to reduce the drag due to lift. Because of the compensating changes in minimum drag and drag due to lift, there was little effect of wing camber on the maximum value of L/D . All other results presented herein were obtained with the cambered-wing arrangement.

The results for various combinations of model components (fig. 4) indicate that the body alone provides a reasonably high slope of the lift curve and a maximum value of L/D of about 4. The addition of the wing causes an increase in lift-curve slope and in minimum drag but a decrease in drag due to lift so that the maximum value of L/D is increased to about 5.2. The results indicate a positive value of C_m at $C_L = 0$ for the configuration either with or without the wing. This effect is probably caused by lifting pressures induced over the canopy. The complete configuration indicates a decrease in stability with increasing lift and, in fact, becomes about neutrally stable in the lift-coefficient range from about 0.2 to 0.5.

Deflection of the elevator (fig. 5) provides reasonably linear increments of C_m . Because of the initial positive value of C_m at $C_L = 0$, positive deflections of the elevator would be required for trim in the lower lift range. Such an arrangement might result in a slight increase in L/D due to trimming since the control deflection required for trimming would provide a positive lift increment. However, because of the neutrally stable region at higher lifts, a slight forward movement of the center of gravity may be necessary.

The effects of various combinations of model components on the sideslip characteristics are presented in figure 6 for several angles of attack. The complete configuration displays a low level of directional stability throughout the angle-of-attack range as a result, primarily, of the large instability of the body alone. In addition to the initially low directional stability, the variation of C_n with β is nonlinear and does in fact reverse with increasing sideslip (fig. 6(a)). The presence of the wing provides a slight stabilizing increment in yawing moment.

The addition of both the wing and the tail provides a positive dihedral effect. With increasing angle of attack the contribution to rolling moment provided by the wing increases while that provided by the tail decreases slightly but the overall effect is a progressive increase in effective dihedral for the complete configuration.

The effects of angle of attack on the sideslip characteristics of the complete model are shown more clearly in figure 7 and the variations of sideslip derivatives with angle of attack for the model with and without the vertical tail are presented in figure 8. The directional stability $C_{n\beta}$ decreases rapidly with increasing angle of attack so that directional instability occurs above $\alpha = 6^\circ$. This decrease in $C_{n\beta}$ is due in part to the increasing instability of the wing-body combination and in part to a loss in vertical-tail effectiveness. The increasing instability of the wing body is characteristic of bodies having far rearward moment centers, whereas the loss in tail effectiveness may be caused by a disturbance created by the inlet lips.

The results also indicate a rapid increase in positive effective dihedral ($-C_{l\beta}$) with increasing angle of attack. This increase in effective dihedral combined with the decrease in $C_{n\beta}$ suggests the need for vertical fin area behind and below the center of moments.

Limited studies of the directional control characteristics (fig. 9) indicate that with increasing α there is a progressive decrease in the ability of the rudder to produce C_n . Deflection of the rudder also causes a substantial increment in adverse rolling-moment coefficient that increases with increasing α . Deflection of the elevator had little effect on the directional control characteristics.

The roll control characteristics (fig. 10) were investigated for differential deflections of $\pm 7.5^\circ$ with elevator deflections of 0° and -25° and for both cases the increment of rolling-moment coefficient obtained was essentially constant with angle of attack. The roll effectiveness was considerably reduced by deflecting the elevator to -25° probably because of a decrease in lift effectiveness of the left elevator at the high total deflection of -32.5° .

CONCLUDING REMARKS

An investigation has been conducted in the Langley 4- by 4-foot supersonic pressure tunnel at a Mach number of 2.01 to determine the stability and control characteristics of a model representative of a

supersonic VTOL airplane. The model had a broad fuselage, small delta wings, and twin vertical tails.

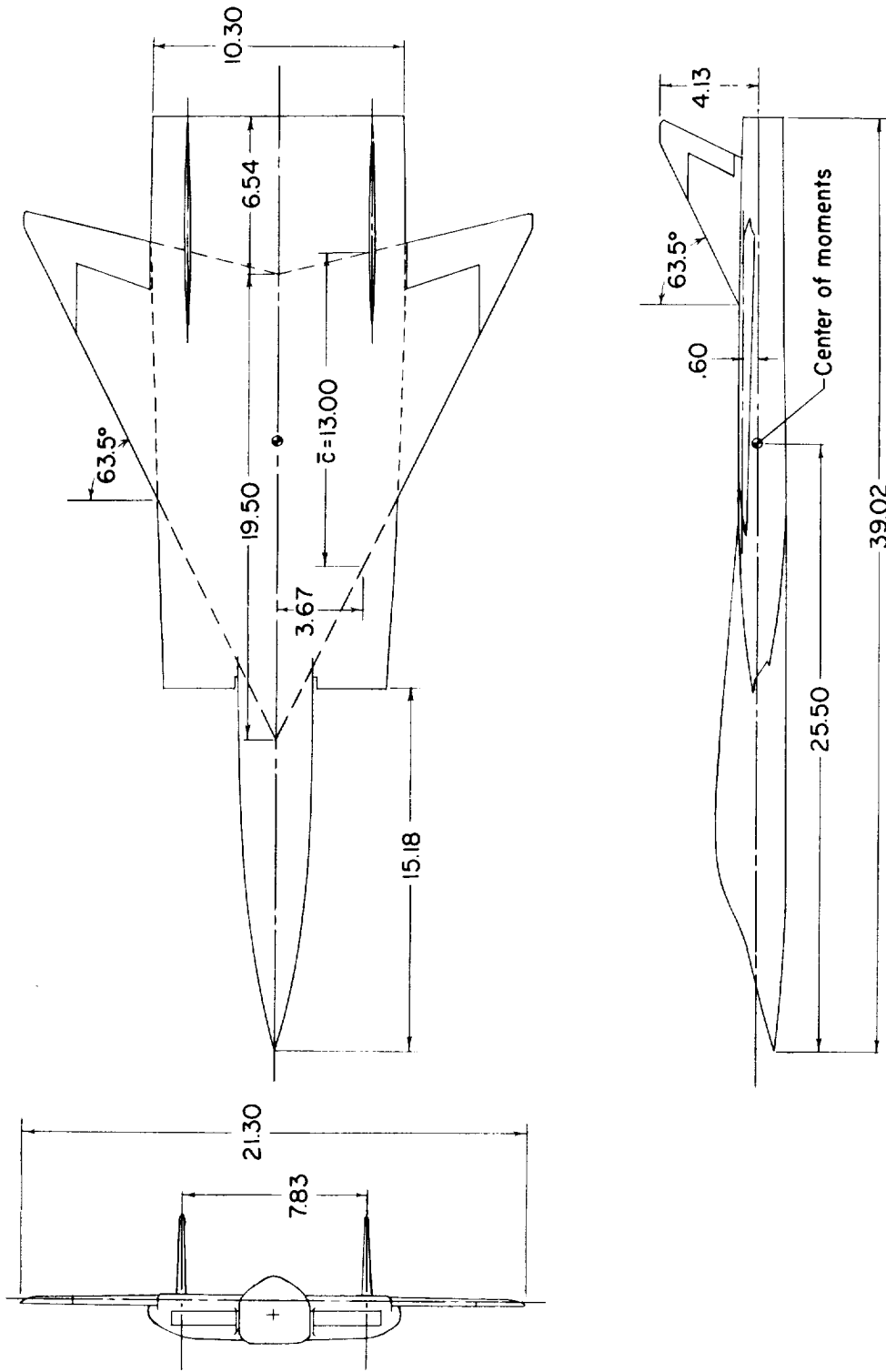
The results indicated that the body alone provides a reasonably high lift-curve slope and a maximum value of lift-drag ratio of about 4. This value was increased to about 5.2 by the addition of the wings. The complete configuration indicated a positive value of pitching moment at zero lift such that positive deflections of the elevator would be required for trimming in the lower lift range. However, because of a reduction in stability at higher lifts, a slight forward movement of the center of gravity may be necessary.

The configuration displayed an initially low value of directional stability that decreased rapidly with increasing angle of attack until directional instability occurred above an angle of 6° . In addition, the configuration had a positive dihedral effect that increased with increasing angle of attack.

Langley Research Center,
National Aeronautics and Space Administration,
Langley Field, Va., October 17, 1960.

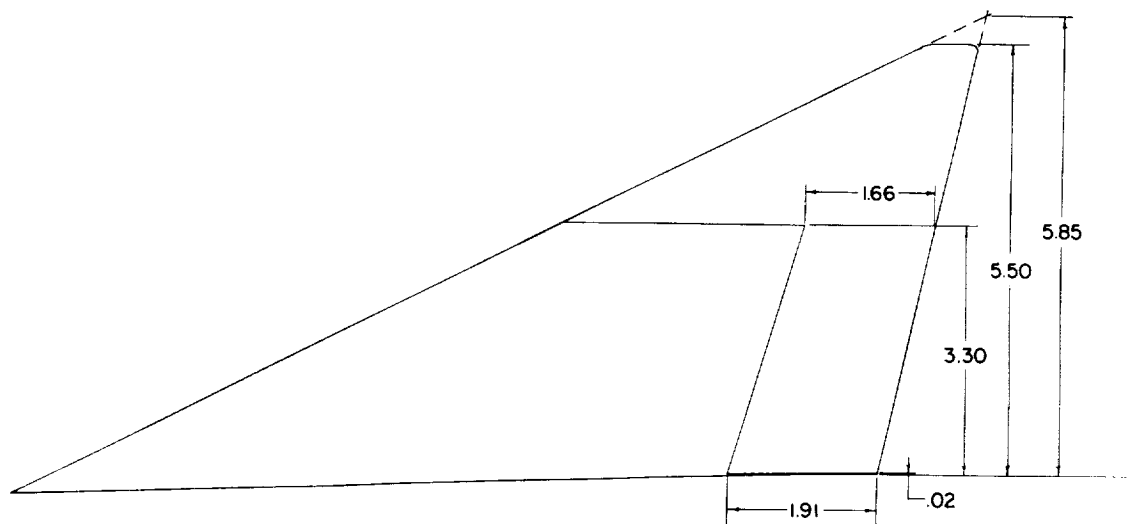
TABLE I.- GEOMETRIC CHARACTERISTICS OF THE MODEL

Wing:	
Span, in.	21.30
Theoretical root chord, in.	19.50
Tip chord, in.	0.62
Mean aerodynamic chord, in.	13.00
Area, sq ft	1.488
Aspect ratio	2.12
Taper ratio	0.032
Leading-edge sweep, deg	63.5
Trailing-edge sweep, deg	13.05
Sweep of quarter-chord line, deg	57.45
Dihedral, deg	0
Incidence, deg	0
Thickness, percent c	3
Elevon area, sq ft	0.322
Body:	
Length, in.	39.02
Maximum width, in.	10.68
Body station for maximum width, in.	36.98
Maximum depth (excluding canopy), in.	1.95
Vertical tail:	
Span, in.	4.13
Root chord:	
Theoretical, in.	7.44
Exposed, in.	6.25
Tip chord, in.	1.09
Leading-edge sweep, deg	63.5
Trailing-edge sweep, deg	25
Vertical-tail area (each):	
Theoretical, sq ft	0.245
Exposed, sq ft	0.172
Rudder area (each), sq ft	0.063



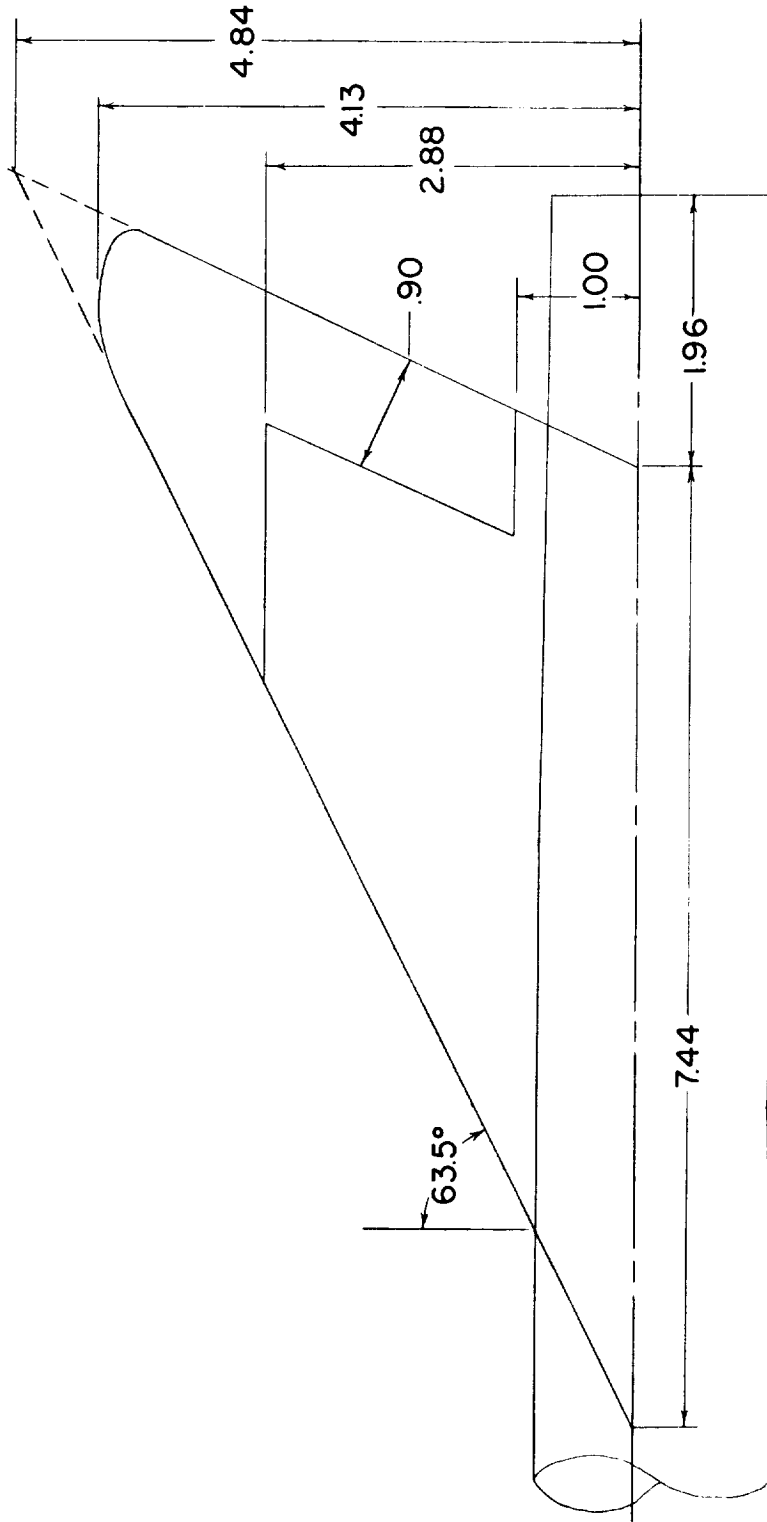
(a) Complete model.

Figure 1.- Details of model. All dimensions are in inches unless otherwise noted.



(b) Exposed wing panel.

Figure 1.- Continued.



(c) Vertical tail.

Figure 1.- Concluded.

CONFIDENTIAL

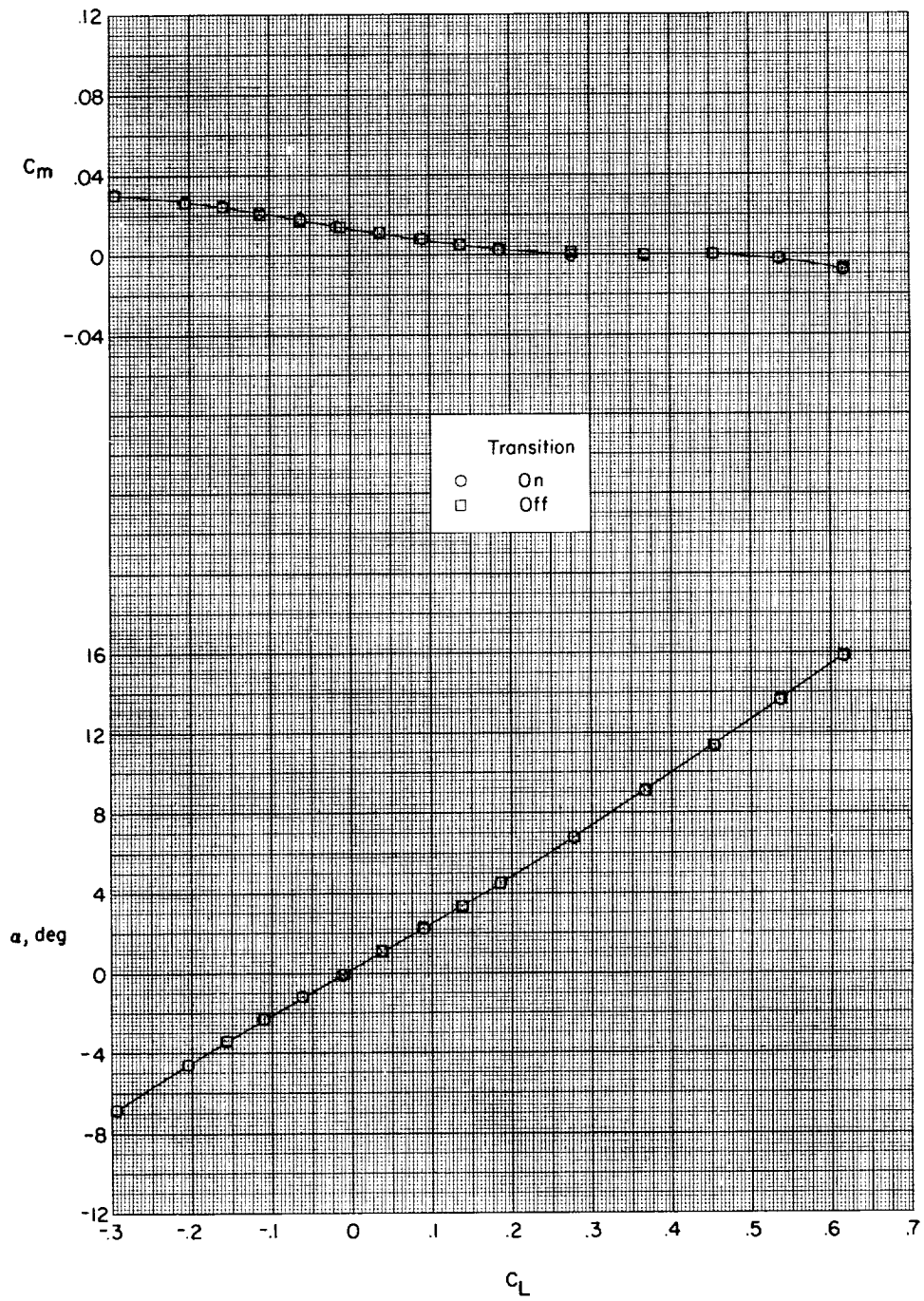
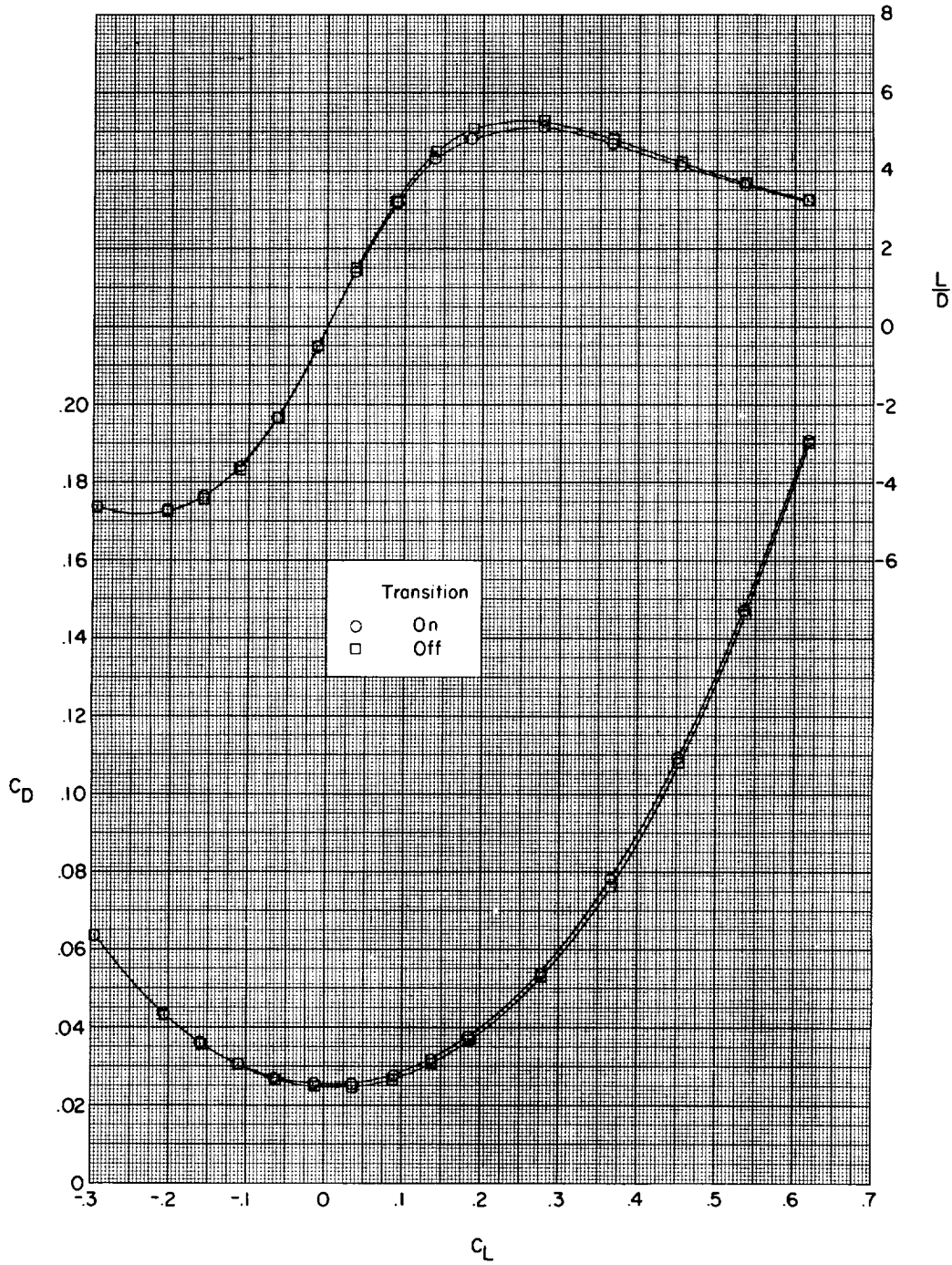
(a) Variation of C_m and α with C_L .

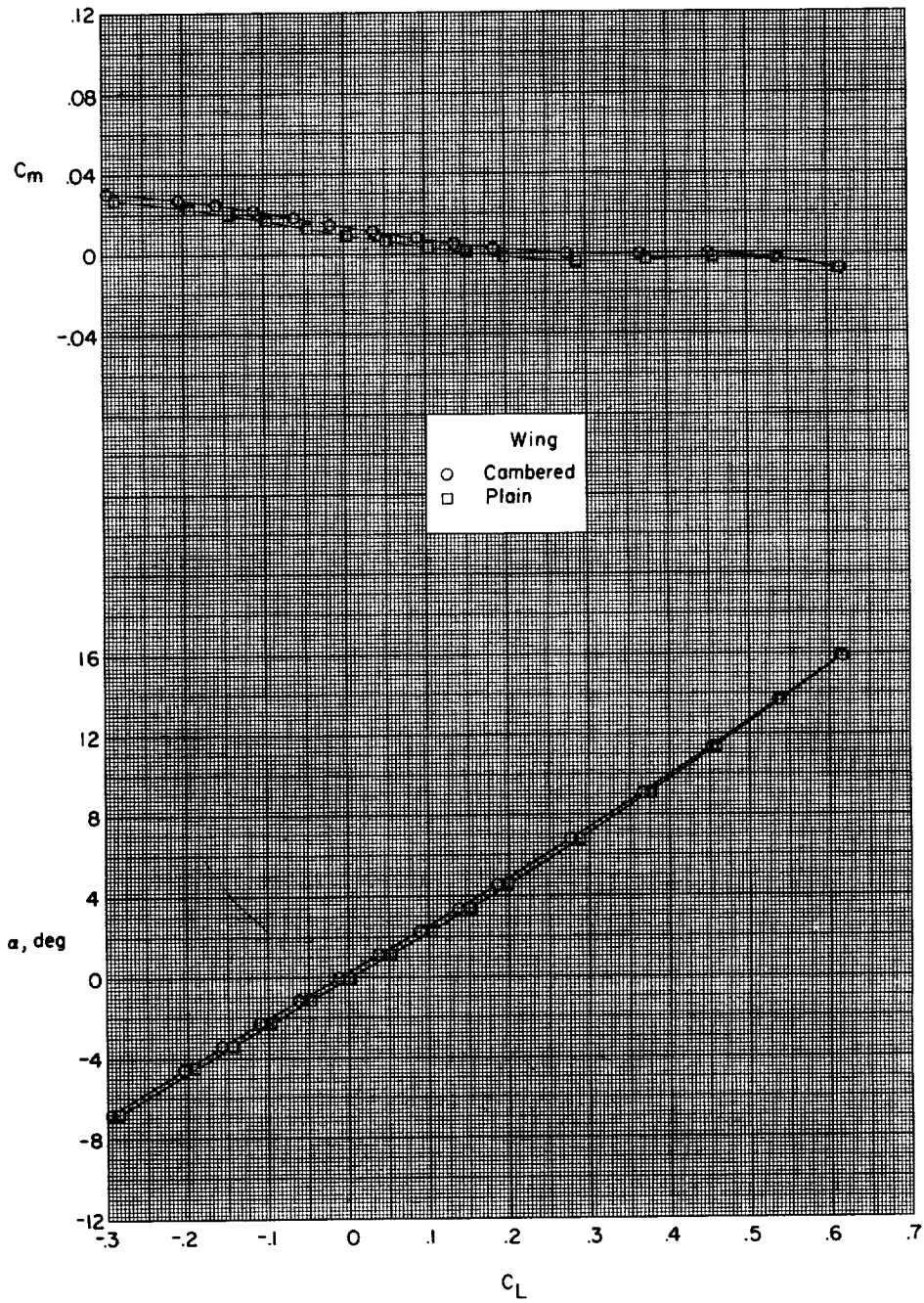
Figure 2.- Effect of transition on aerodynamic characteristics in pitch.

CONFIDENTIAL



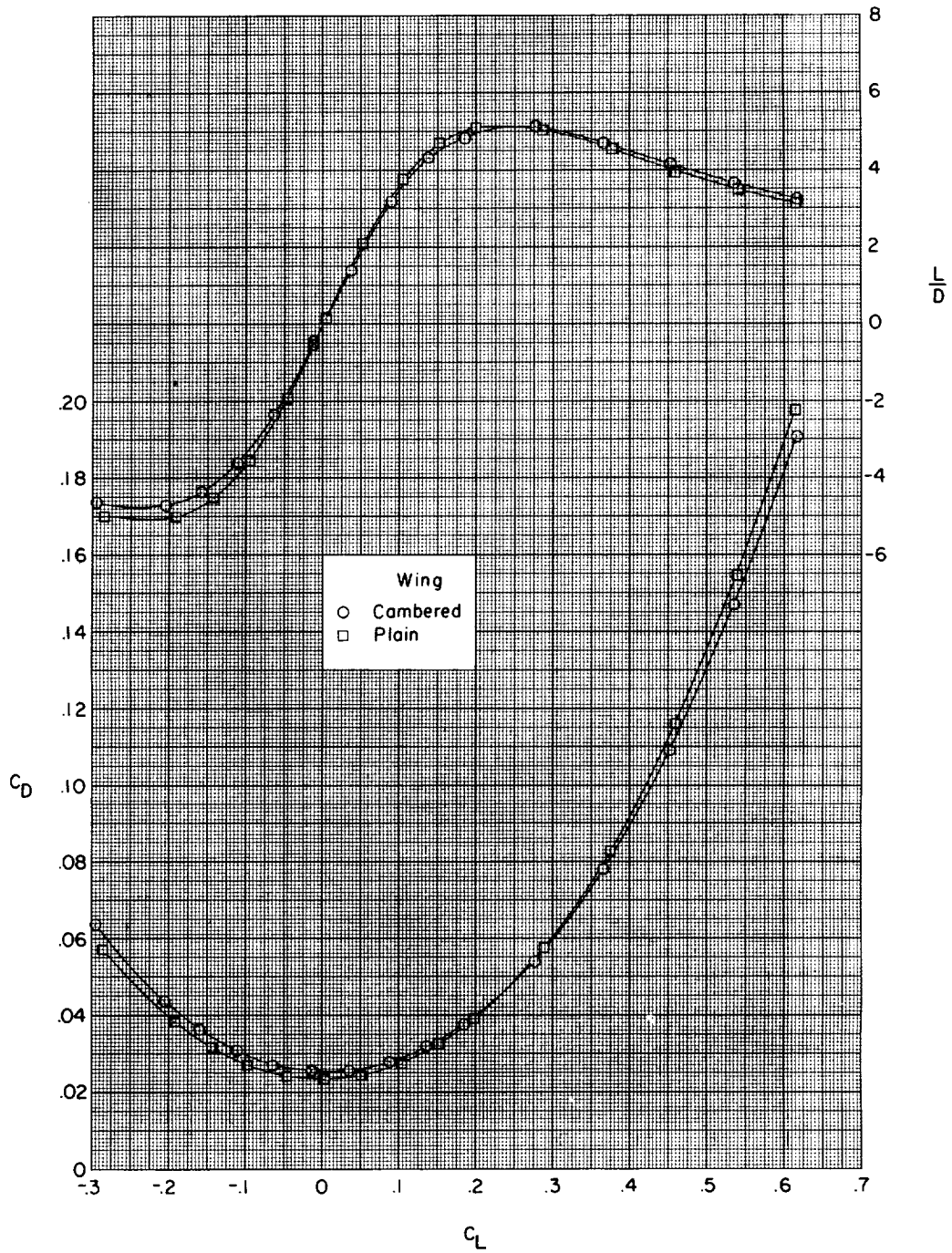
(b) Variation of L/D and C_D with C_L .

Figure 2.- Concluded.



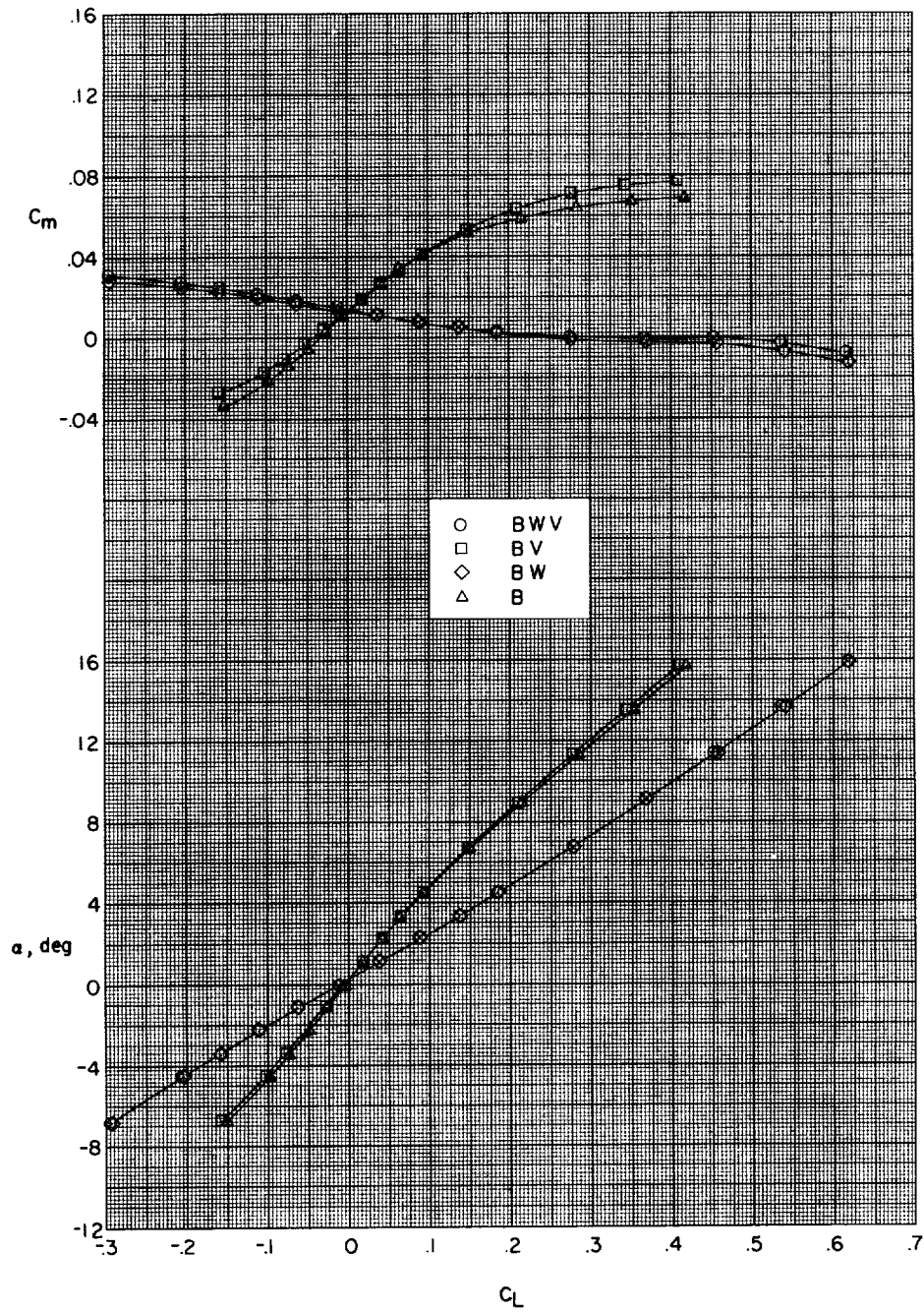
(a) Variation of C_m and α with C_L .

Figure 3.- Effect of wing camber on aerodynamic characteristics in pitch.



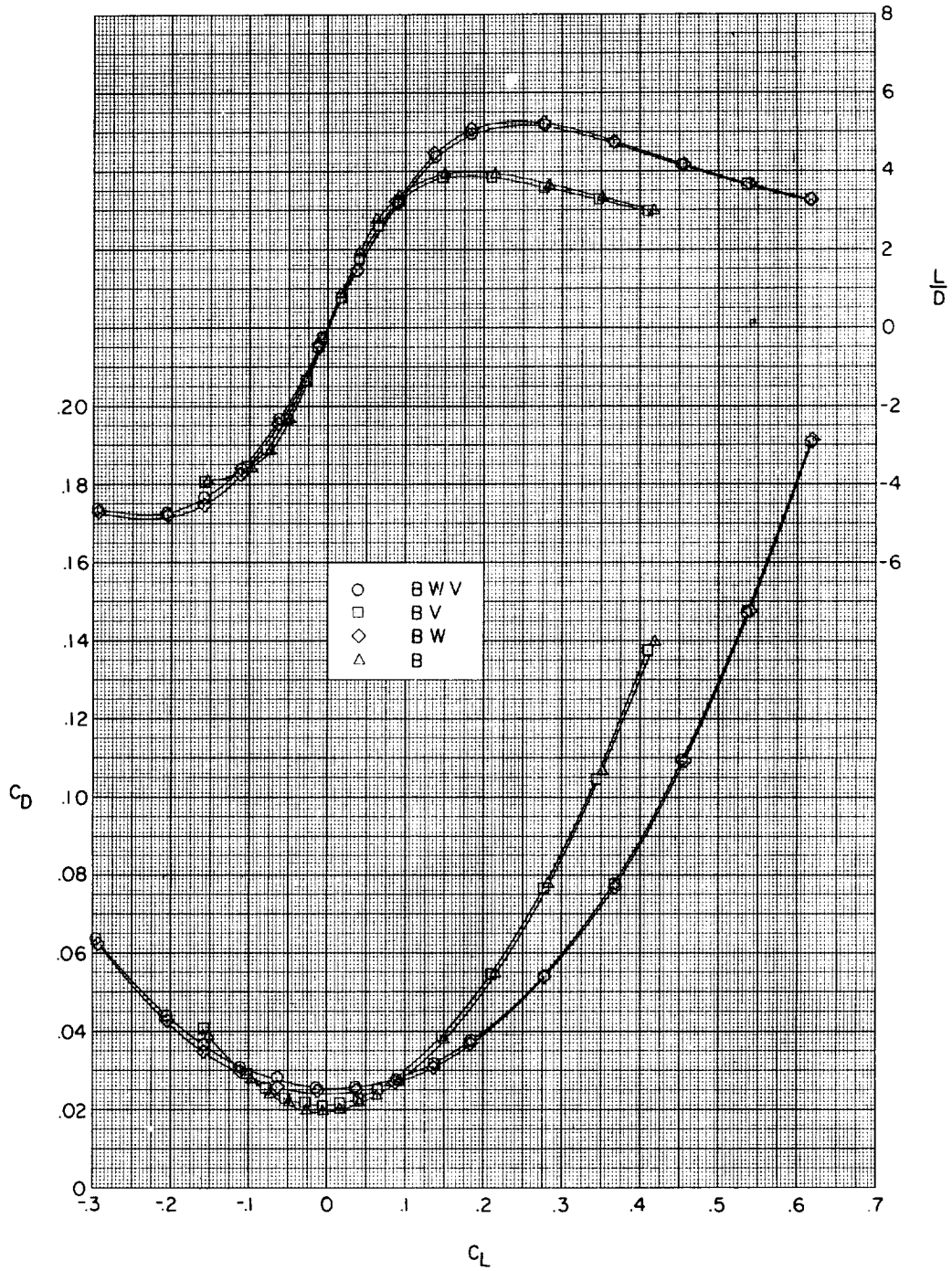
(b) Variation of L/D and C_D with C_L.

Figure 3.- Concluded.



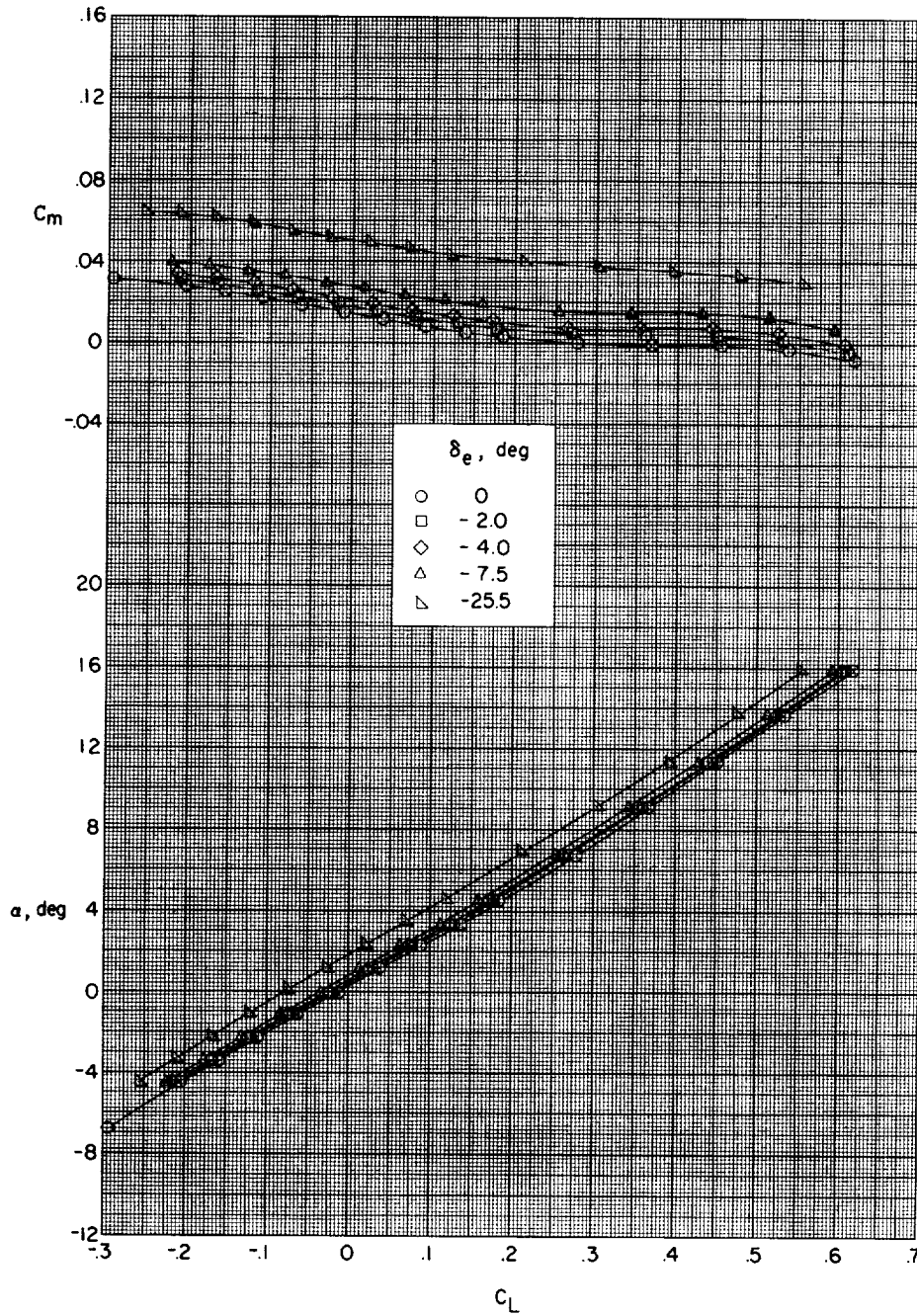
(a) Variation of C_m and α with C_L .

Figure 4.- Effect of model components on aerodynamic characteristics in pitch.



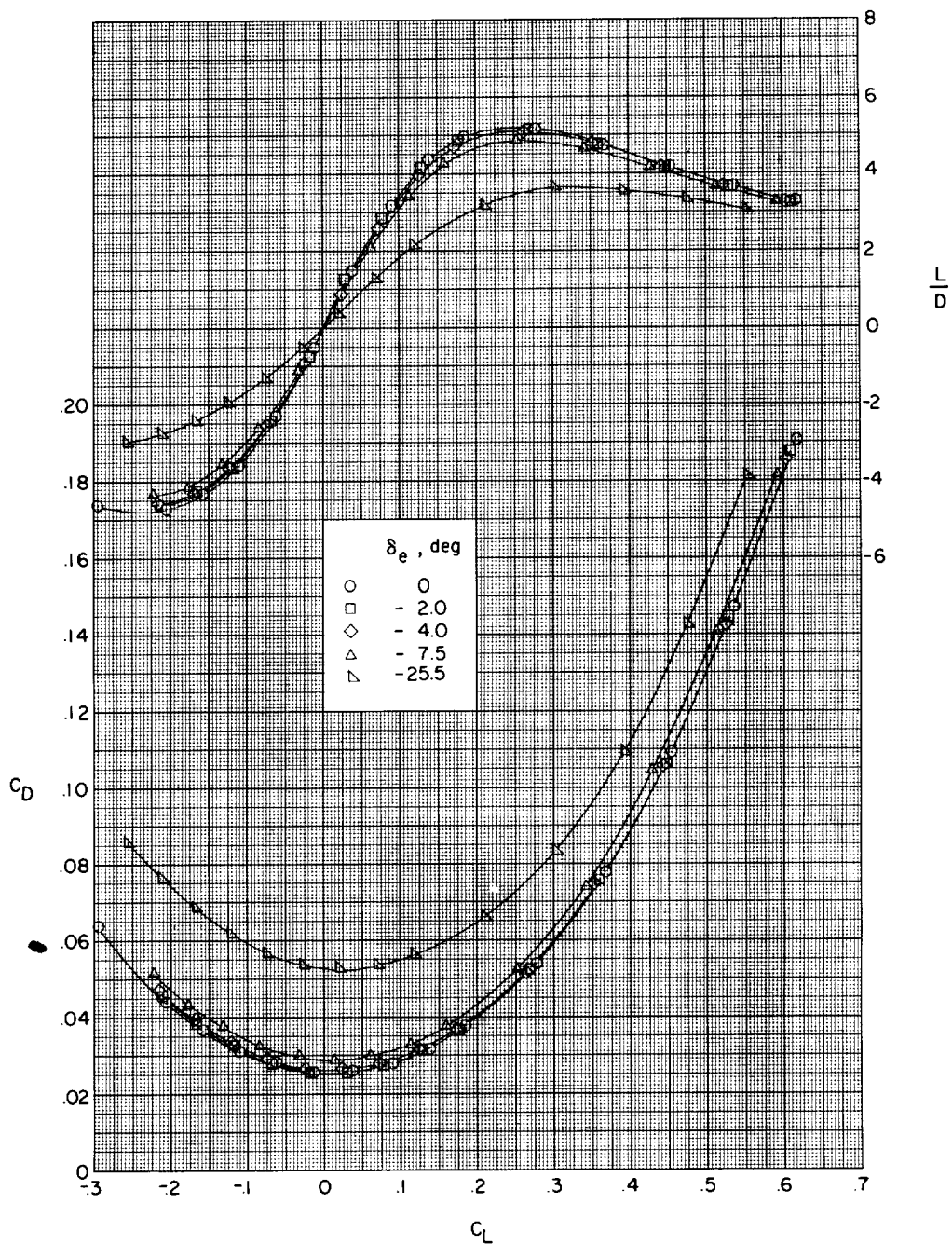
(b) Variation of L/D and CD with CL.

Figure 4.- Concluded.



(a) Variation of C_m and α with C_L .

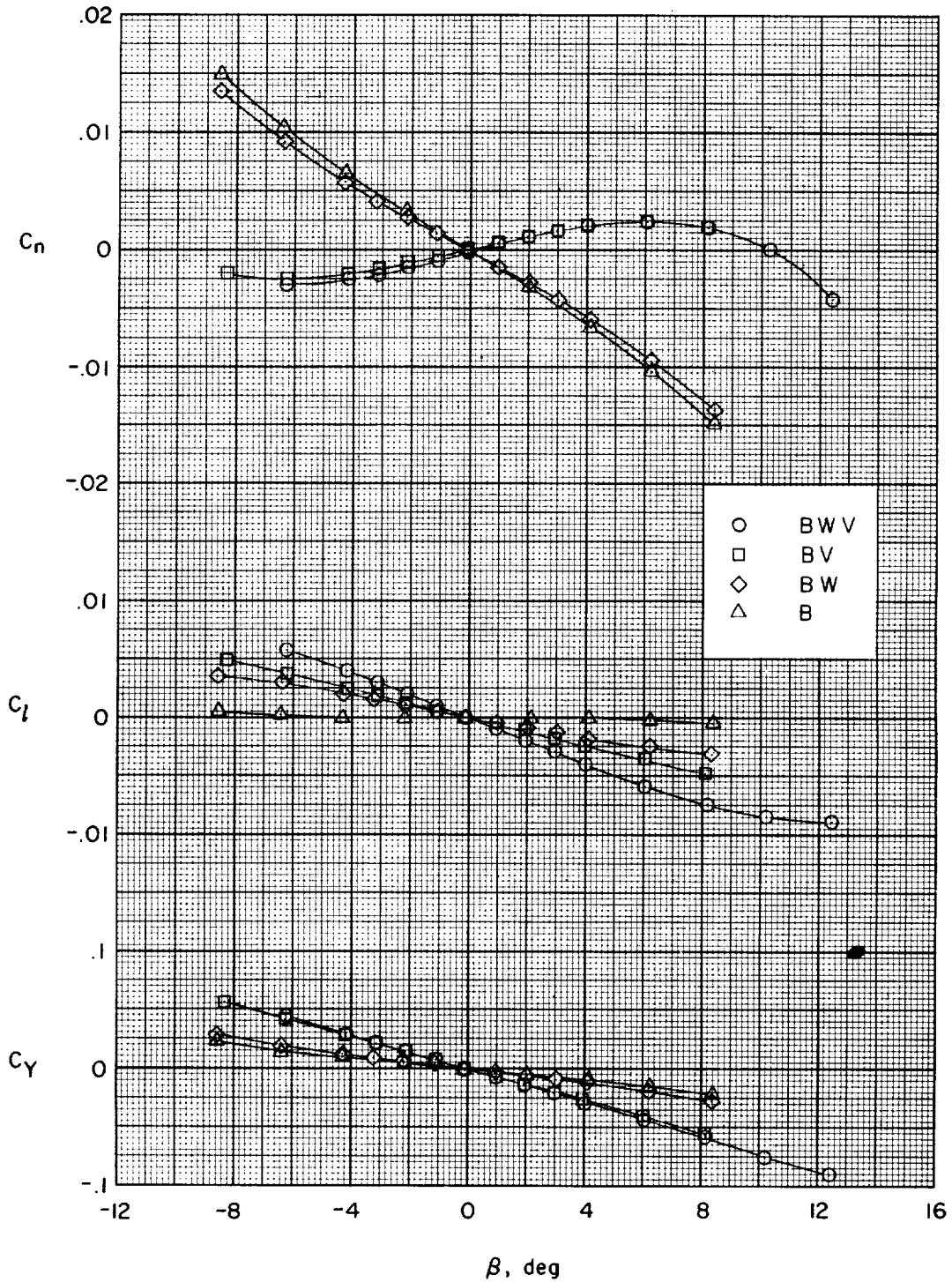
Figure 5.- Effect of elevator deflection on the aerodynamic characteristics in pitch.



(b) Variation of L/D and C_D with C_L .

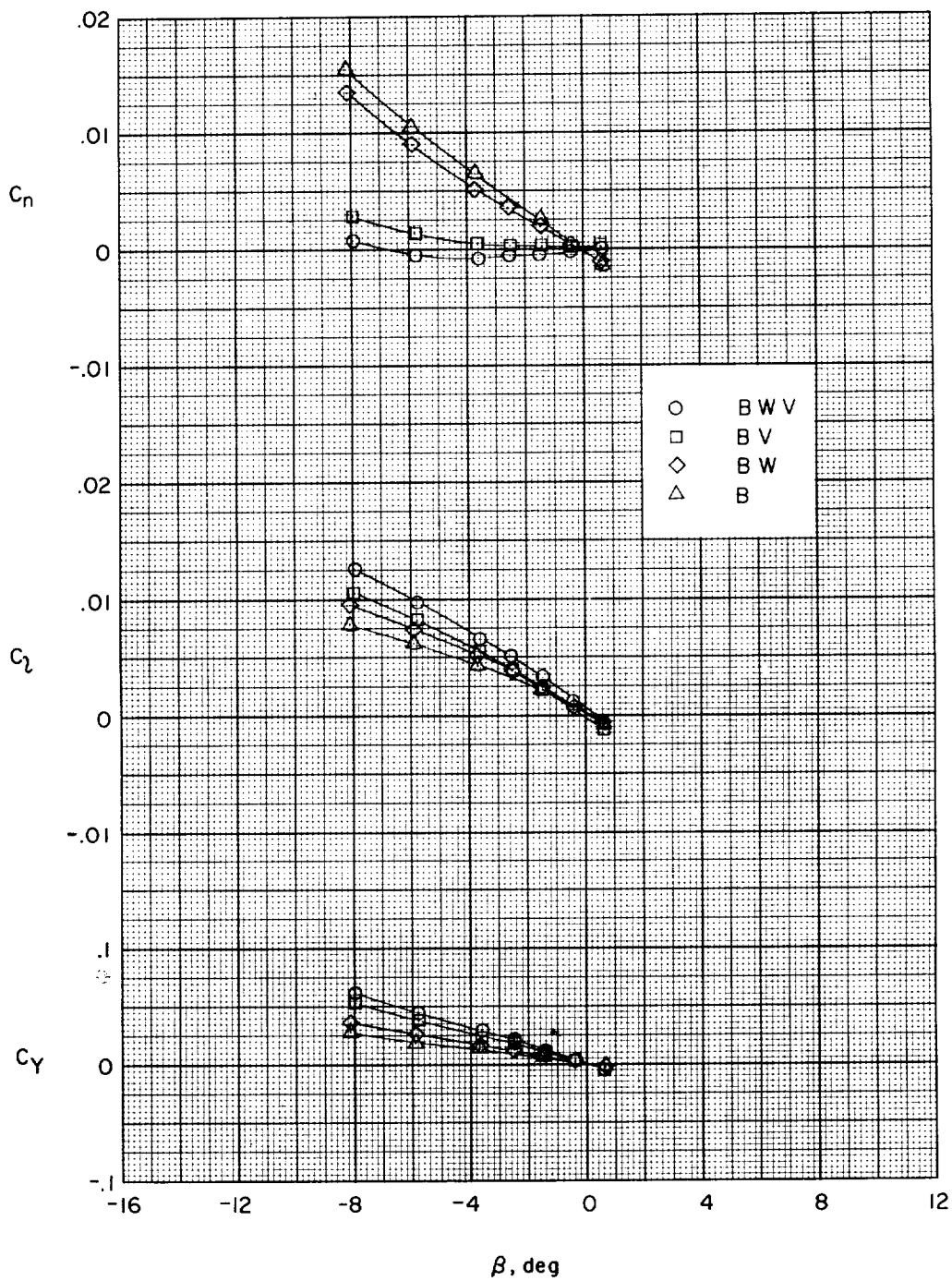
Figure 5.- Concluded.

CONFIDENTIAL



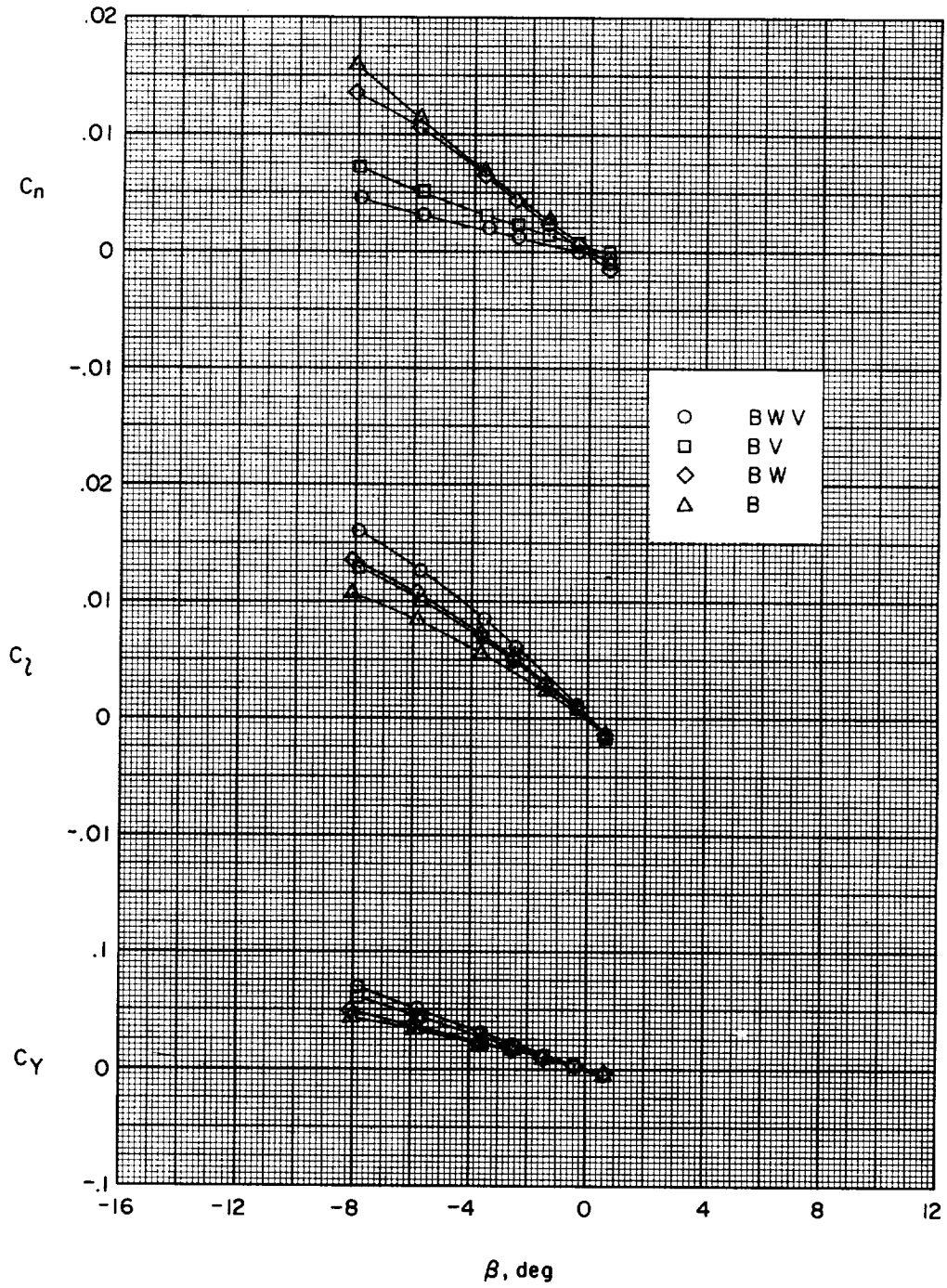
(a) $\alpha = -0.5^\circ$.

Figure 6.- Effect of model components on aerodynamic characteristics in sideslip for various angles of attack.



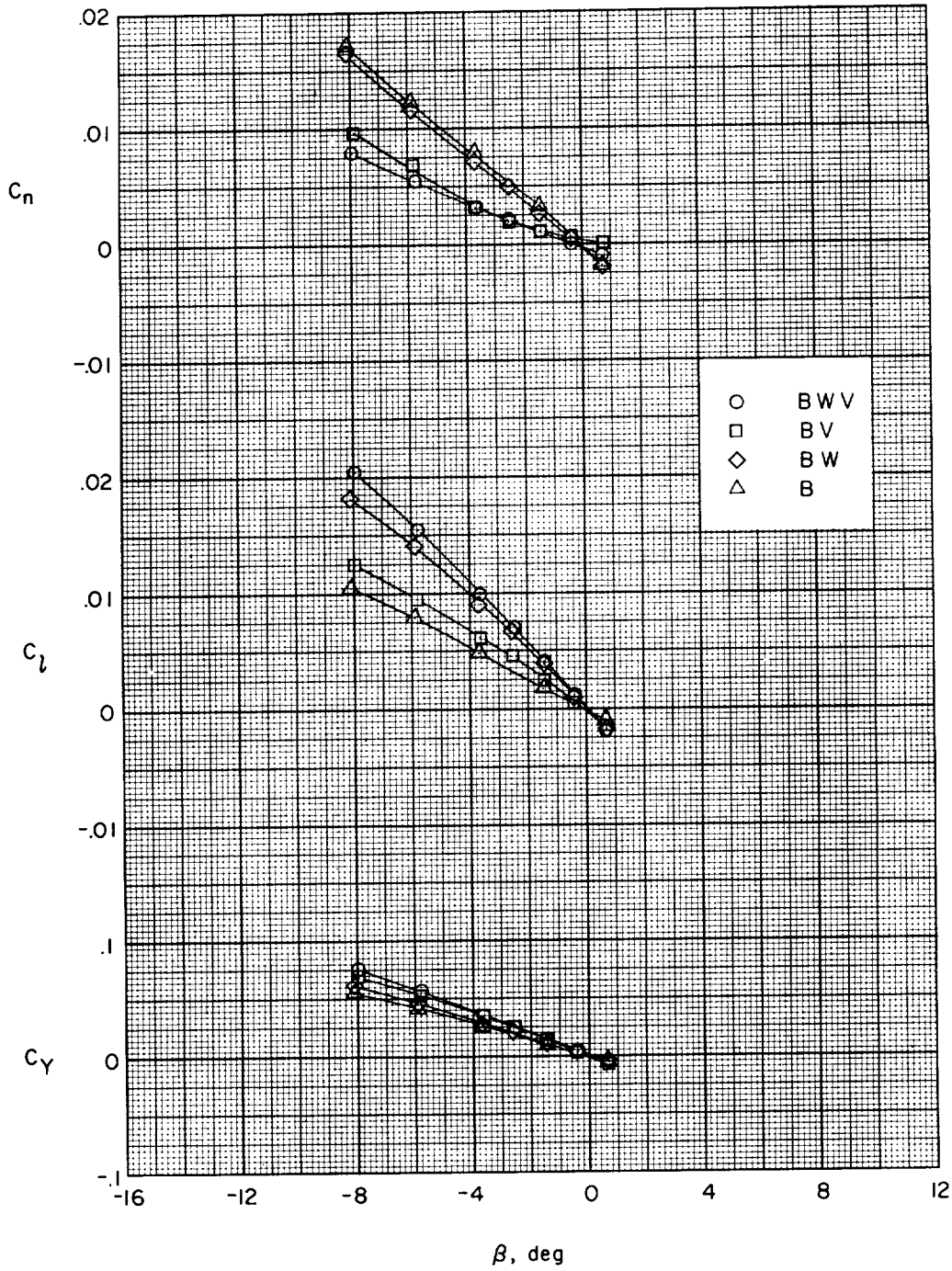
(b) $\alpha = 4.8^\circ$.

Figure 6.- Continued.



(c) $\alpha = 9.3^\circ$.

Figure 6.- Continued.



(d) $\alpha = 13.8^\circ$.

Figure 6.- Concluded.

CONFIDENTIAL

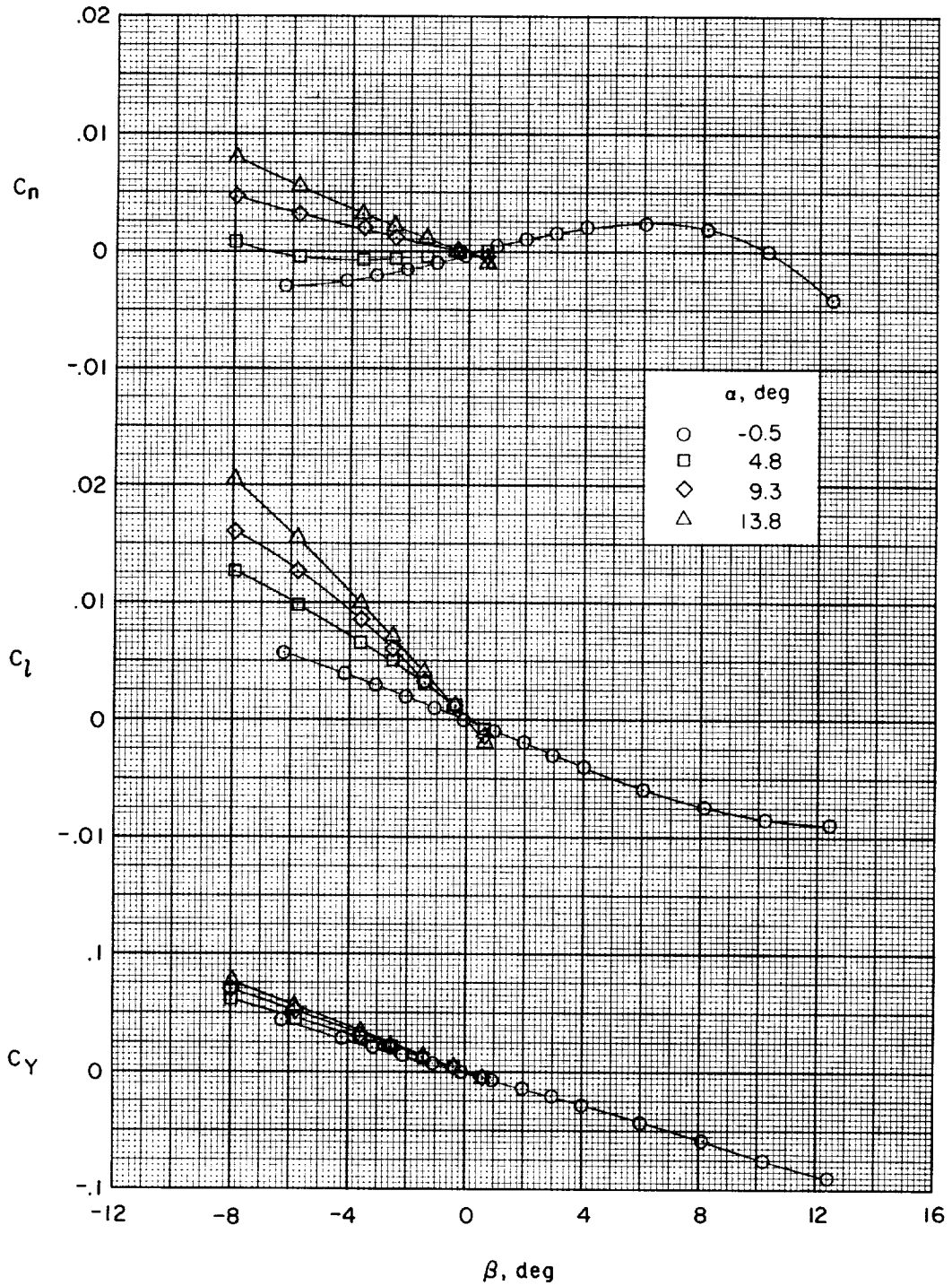


Figure 7.- Effect of angle of attack on aerodynamic characteristics in sideslip. Complete model.

CONFIDENTIAL

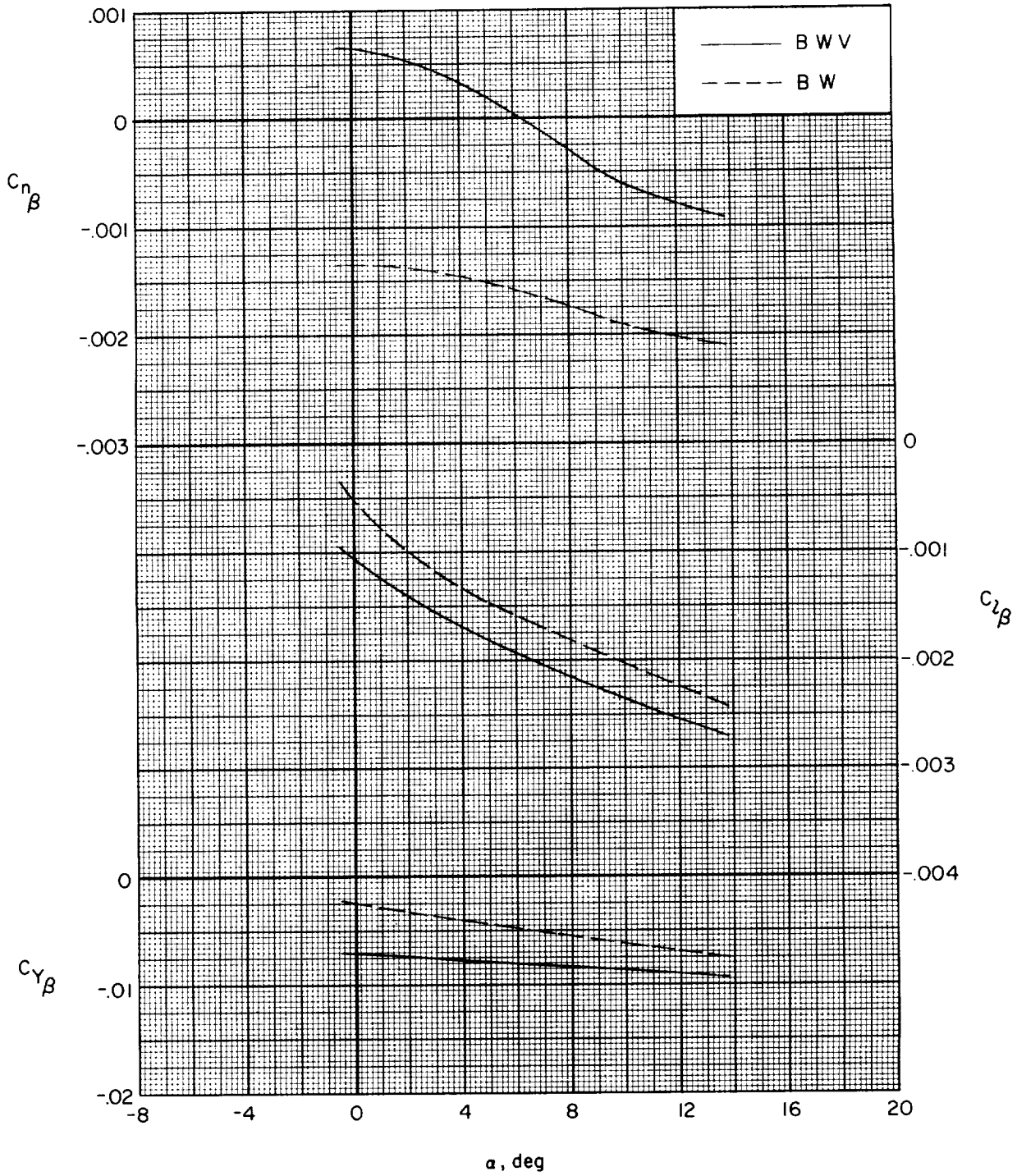


Figure 8.- Variation of sideslip derivatives with angle of attack.

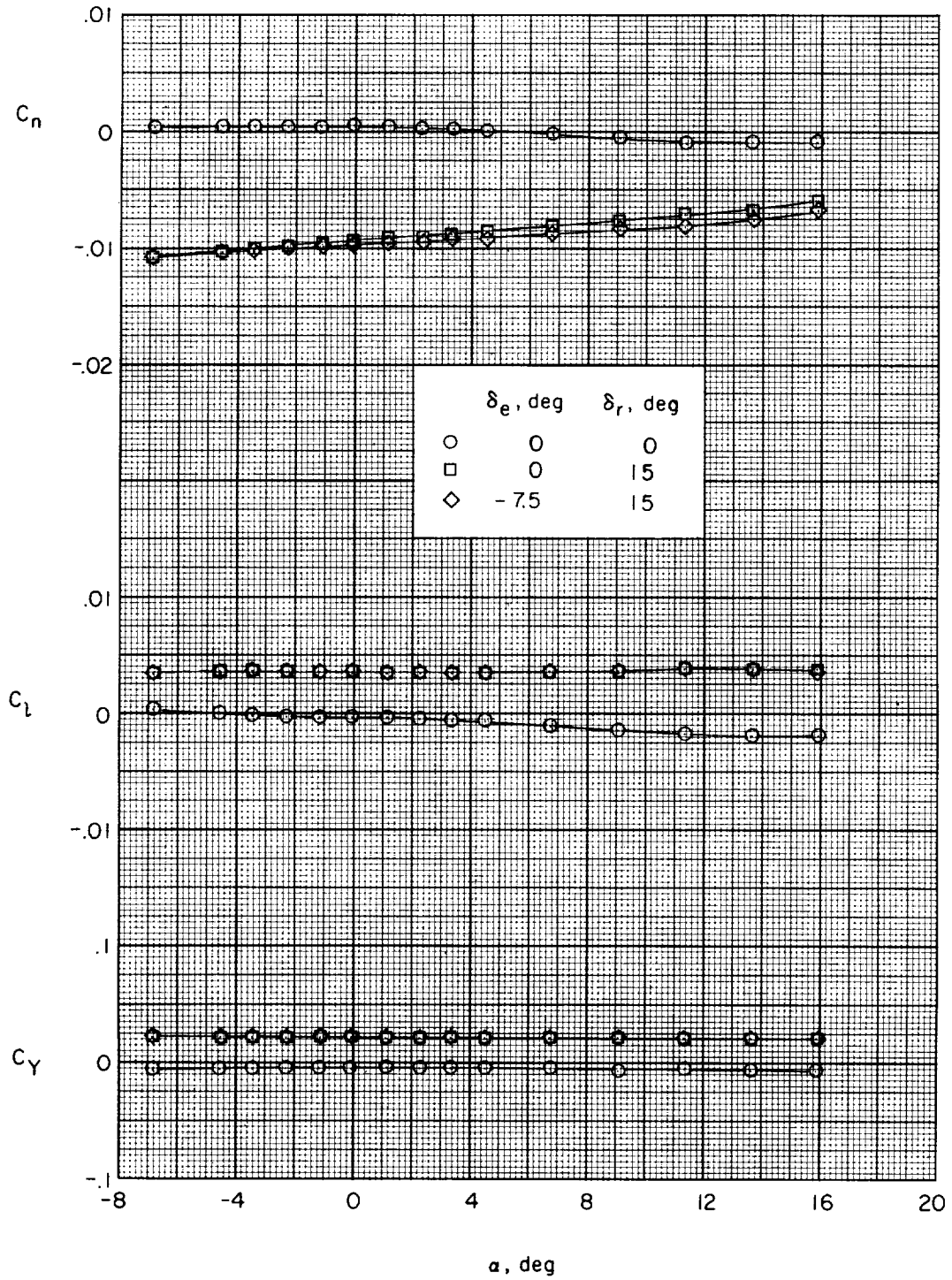


Figure 9.- Directional control characteristics.

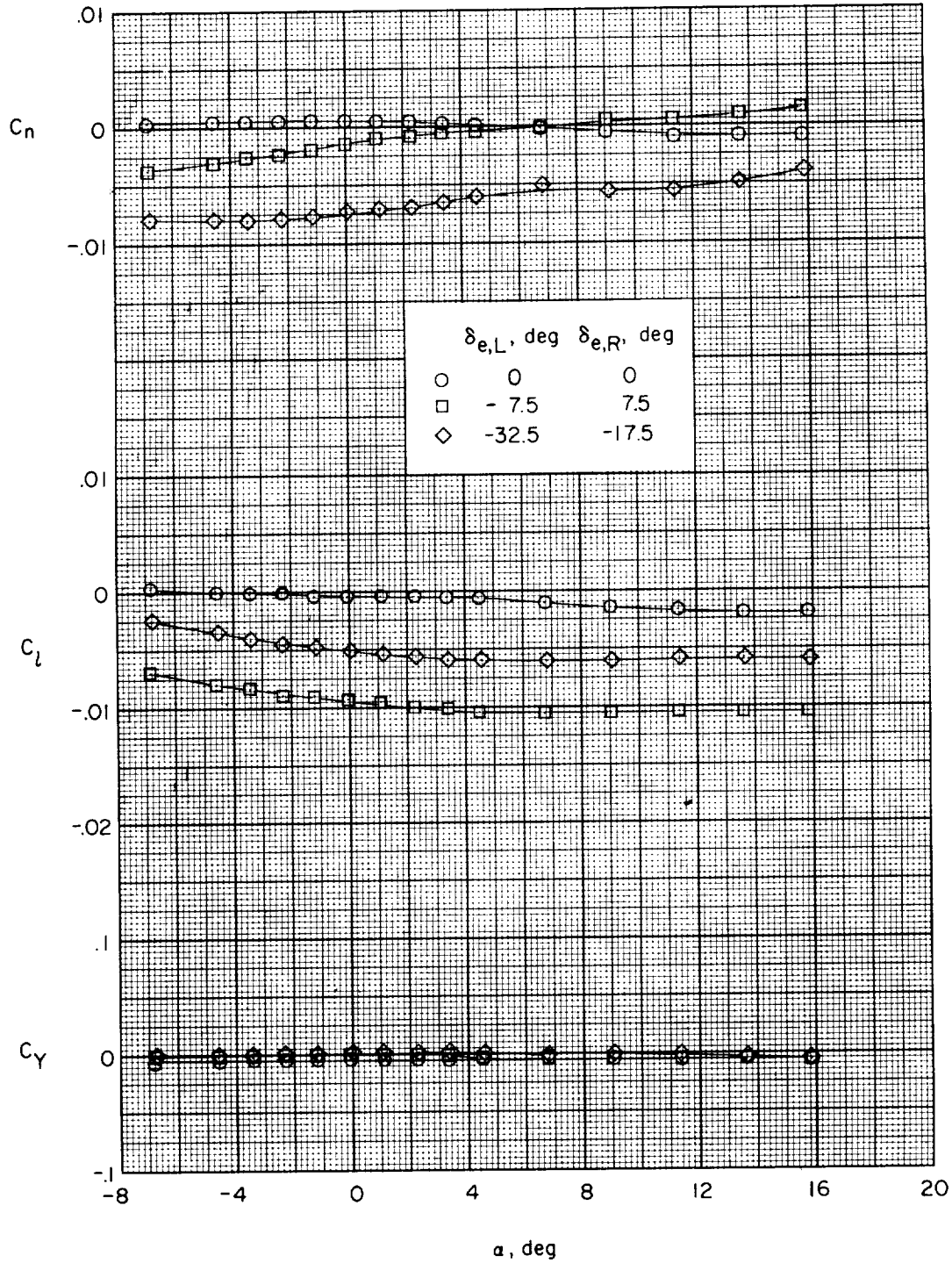


Figure 10.- Roll control characteristics.

DECLASSIFIED

CONFIDENTIAL

CONFIDENTIAL